Journal of ELECTRICAL ENGINEERING, VOL 55. NO 10/S, 2004, 124-127

CRITICAL PARAMETERS IN CURRENT EVALUATION BY MAGNETIC FIELD MEASUREMENTS

Oriano Bottauscio[*] — Mario Chiampi[**] — Gabriella Crotti[*] — Mauro Zucca[*]

Current evaluation by magnetic field measurements can be usefully adopted when current direct measurements are not feasible. The same approach is also relevant to the determination of the turn number in a coil in which the electrical current is known. To this end, the solution of an inverse problem is required, entailing the knowledge of the actual disposition of the sources (cables, bar, coils, etc.). The uncertainty in the evaluation of the unknown quantities (current amplitude, turn number, etc.) is affected by several factors like the characteristics of the probes, their dimension and position, the source geometry. All these aspects and the methods for minimizing the measurement uncertainties are discussed in the present work using a suitable simulation environment.

Keywords: current measurement, probe array, inverse problem.

1 INTRODUCTION

The evaluation of currents or, more in general, magnetomotive forces (mmf) by magnetic field measurements can be usefully adopted when a reduced space or a high number of conductors do not allow a direct experimental procedure. The same approach is also relevant in the power measurement when highly distorted current waveforms make unreliable the employment of amperometric transformers.

The estimation of the current evolution from field measurements requires the solution of an inverse problem, entailing the knowledge of the actual arrangement of the sources (cables, bars, coils, etc.). Thus, the uncertainty associated to the estimated value of the unknown quantities (current waveform, turn number, etc.) becomes dependent, not only on the measurement uncertainties of the field meter, but also on the numerical process for the solution of the inverse problem.

The paper first presents a method for the fast solution of the inverse problem; then the attention is devoted to the analysis of the uncertainty contributions associated to the current estimate due to the sensor accuracy and dimension and to the presence of a stray field (external disturbances). The error introduced by the computational procedure in the current evaluation is also discussed. Eventually, suggestions are given in order to reduce the uncertainty contributions affecting the final results. The paper is completed by some examples of application of the proposed procedure.

2 DESCRIPTION OF THE METHOD

The estimation of the source characteristics from magnetic field measurements is usually performed by optimisation algorithms, which can require significant processing time. The method here proposed, taking advantage of the knowledge of the source position, is very simple and fast and it enables an on-line elaboration of the signals. The signals are expressed as a function of the magnetomotive forces through the Biot-Savart law and then are processed by a numerical algorithm, based on the Singular Value Decomposition (SVD) procedure. The measurement system makes use of a probe array with more sensors than unknowns, in order to improve the technique efficiency. Some examples, performed by a numerical simulation of the measurement system, put in evidence the method capability of accurately reproducing the current (or mmf) behaviour.

2.1 Source simulation

The first step of the proposed procedure is the definition of a relationship between source (current) and field (magnetic flux density). Under the assumption of 2D linear magnetic field, this link is obtained by the Biot–Savart law:

$$\mathbf{B}(P_s) = \mu_0 \sum_{k=1}^{K} \int_{\Omega_k} \mathbf{J}_k \times \nabla \psi \, \mathrm{d}\omega \tag{1}$$

where ψ is the Green function, P_s is the measurement point, K is the number of conductors, having area Ω_k and vector current density $\mathbf{J}_k$. In such a way, the indication b_m of the generic m-th probe can be expressed as a function of the unknown currents (or mmf) s_k:

$$b_m = \sum_{k=1}^{K} \alpha_{mk} s_k \tag{2}$$

In order to compute the coefficient of Eqn. (2), after the definition of the workspace dimensions and of the conductor and sensor arrangement, the following steps are performed:

1) a unitary current is assigned to each conductor at a time and the indication of each probe sensor, which represents the coefficient α_m, is computed;
2) assuming the actual current values, the relative probe indication b_m, that is the right-hand side of Eqn. (2), is computed.

The computational procedure is performed by a numerical code able to handle any shape of conductor cross-section.

The execution of the previous operations leads to the solution of the algebraic system :

[*] Istituto Elettrotecnico Nazionale G. Ferraris strada delle Cacce 91, I-10135 Torino (Italy) - [**] Dipartimento di Ingegneria Elettrica Industriale, Politecnico di Torino, corso Duca degli Abruzzi 24, I-10129 Torino, Italy, zucca@ien.it

ISSN 1335-3632

$$[\mathbf{A}]\cdot[\mathbf{S}]=[\mathbf{B}] \tag{3}$$

having M (number of probes) equations with K (number of currents) unknowns. For the purpose of improving the efficiency of the proposed technique, M is assumed to be always greater than K.

The solution of system (3) can become inaccurate when some equations are close to be linearly dependent, that is when two or more sensors are in very close positions and provide similar indications. A quality index (*PI*) of the solution can be obtained by analysing the minor determinants of order K of matrix **A**; the highest the value of *PI*, the higher the reconstruction accuracy. This index allows a comparison of different probe array positions and the exclusion of the configurations with the lower *PI* values, which lead to less accurate current estimations.

2.2 SVD Algorithm

The SVD algorithm is applied to algebraic systems, as (3), having more equations than unknowns [1]. Given the system matrix **A**, the algorithm computes its singular value decomposition according to:

$$\mathbf{A}=\mathbf{R}\cdot\mathbf{W}\cdot\mathbf{V}^{\mathbf{T}} \text{ that is: } \alpha_{mk}=\sum_{j=1}^{K} w_j\cdot r_{mj}\cdot v_{kj} \tag{4}$$

The least-squares solution vector **S** is given by:

$$\begin{pmatrix}\mathbf{S}\end{pmatrix}=\begin{pmatrix}\mathbf{V}\end{pmatrix}\cdot\begin{pmatrix}diag(1/wj)\end{pmatrix}\cdot\begin{pmatrix}\mathbf{R}^{\mathbf{T}}\end{pmatrix}\cdot\begin{pmatrix}\mathbf{B}\end{pmatrix} \tag{5}$$

2.3 Stray fields

The presence of stray magnetic fields should be taken in due consideration, because they affect the sensor indications and consequently the current reconstruction. Stray magnetic fields in a frequency range from 0 to 10 kHz are usually generated by sources located far from the measurement point. So, these fields can be supposed uniform on the measurement area. This last assumption allows one to take into account their presence by introducing an additional unknown in the relation between field and sources according to:

$$b_m=\sum_{k=1}^{K}\alpha_{mk}s_k+b_0 \tag{6}$$

where b_0 is the unknown stray field component. The structure of system (5) is unchanged, but an additional unknown is added to column vector **S**.

3 UNCERTAINTY AND POSITION PARAMETERS

The predicted values of currents (or m.m.f.) are affected by measurement uncertainties due to the probes (averaging error and instrumental uncertainty). In the following, these components will be investigated and their effect on current evaluation will be discussed, analysing their propagation.

3.1 Averaging error

The averaging error is the deviation between measured and actual field due to the finite dimension of the field sensors and it arises where the field distribution is strongly non-uniform [2]. The sensor centre is placed on a given measurement point *P*, where the *i*-component of the magnetic field density, called b_{PAi} is assumed as the actual value. Stated the sensor area Ω, the error is given by:

$$\varepsilon_{avgPi}=\frac{\frac{1}{\Omega}\int_{\Omega} b_i\cdot d\omega-b_{PAi}}{b_{PAi}}=\frac{b_{m,i}-b_{PAi}}{b_{PAi}} \tag{7}$$

Error $\varepsilon_{avgP\,i}$ reduces (or vanishes) if the probe sensors are positioned where the magnetic field is more uniform.

3.2 Uncertainty evaluation

Under the hypothesis of high values of index *PI*, two uncertainty contributions associated to the current estimate have been identified. The uncertainty contribution $\boldsymbol{u}_1$ due to averaging error is evaluated from the computation of the relative deviation between the measured ($\mathbf{S}_m$) and the actual ($\mathbf{S}_a$) current (or mmf) values. The vector $\mathbf{S}_m$ is obtained by applying relation (5) where the elements of vector **B** are the sensor indications $b_{m,i}$.

The vector of the uncertainty contribution $\boldsymbol{u}_2$ due to the sensor accuracy is computed starting from the uncertainty vector $\boldsymbol{u}_s$ of the sensor indications and applying the uncertainty propagation law to relation (5):

$$\begin{bmatrix}u_2^2\end{bmatrix}=\begin{bmatrix}\mathbf{Q}^2\end{bmatrix}\cdot\begin{bmatrix}u_s^2\end{bmatrix} \tag{8}$$

where $\mathbf{Q}=(\mathbf{V}\cdot\mathbf{W}^{-1}\cdot\mathbf{R}^{\mathbf{T}})$.

The expanded uncertainty $\boldsymbol{U}$ associated to the reconstructed value of *k*-th current is given by:

$$U_k=2\sqrt{u_{1,k}^2+u_{2,k}^2} \tag{9}$$

having assumed a coverage factor $K_F = 2$ corresponding to a confidence level of ~95%.

4 APPLICATION EXAMPLES

In the following, two examples of application are presented. The first one concerns the case of a go-and-return system constituted of four bars, whereas the second example refers to three cables supplied by a balanced three phase current system. In all the cases, N single-axis sensors with dimension equal to 1 cm are disposed on a rectangular grid to constitute an array. The sensors are arranged to form couples constituted of two concentric

sensors oriented along x and y directions respectively. The accuracy of the sensors is assumed to be 0.1 %.

4.1 Go and return system

The system is constituted by four bars, each of them supplied with a 100 A current. The four currents, assumed as unknowns, are determined through the proposed method. First the analysis is focused on the influence of the index *PI* on the accuracy of the current estimate. To this end, an array composed of six sensors is placed in different positions (from #1 to #5), as sketched in Fig. 1.

In a first step, the averaging error of the sensor is neglected, assuming as measured value the magnetic flux density in the centre of the probe. The obtained results are summarized in Table I, which reports the values of the estimated currents for the five considered configurations, together with the corresponding *PI* value. It is evident how a low value of index *PI* (configuration #5) leads to significant deviations between actual and computed values. The best estimates are found for configuration #3, having the highest value of *PI*. The worst results are obtained in configuration #5, where the field is more uniform and similar indications are given by the different sensors. It must be underlined that varying the structure of the array (e.g. the number of sensors), the *PI* indexes related to different arrays are no more comparable.

Once identified the configuration associated to the highest *PI* value (#3), the influence of the sensor number is investigated. Table II reports the maximum elements of the vectors $\boldsymbol{u_1}$ and $\boldsymbol{u_2}$ expressed as relative standard uncertainties in the case of 6, 8 and 12 sensors. As expected, the use of an array with a higher number of sensors leads to lower measurement uncertainties. Same considerations are valid in presence of a significant stray field with an amplitude up to several percents of the sensor indications, as shown in Table III for arrays with 8 and 12 sensors. For all the analysed configurations the uncertainty component u_1 results always negligible with respect to u_2. The low value of the uncertainty associated to the size averaging effect makes less critical the positioning of the sensor in regions with high field gradient.

4.2 Three phase system

The considered three-phase system is constituted of three cables (diameter 45 mm), with a distance of 80 mm between their centres. Three arrays (#6, #7 and #8) with the same number of sensors (N=12), but different distance between them (and therefore different array dimension) have been taken into consideration (Fig. 2); the array configuration #6 has the same dimensions as those previously used for the go and return system. The uncertainty component $\boldsymbol{u}_1$ is again found to be negligible with respect to $\boldsymbol{u}_2$. The results of the analysis performed on configurations #6, #7 and #8 with and without the stray field are presented in Table IV.

Increasing the array dimensions, and consequently the distance between the sensors, an improvement of the results is found, in particular when the stray field is present. However, in the case of arrangement #6, the comparison with the data obtained with same array applied to the go-and-return source, which is characterized by a reduced size with respect to the array, shows an increase of the uncertainty level.

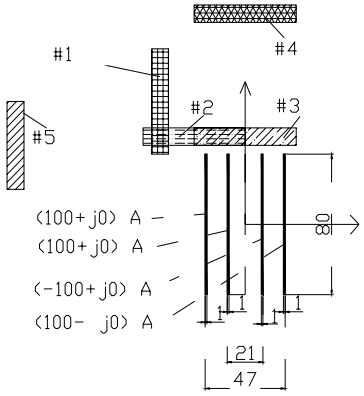

Fig. 1. System and probe area location (dimensions in millimetres)

Table 1. Results for the 6 sensor array

Case	*PI*	I_1 (A)	I_2 (A)	I_3 (A)	I_4 (A)
Actual values	-	100.00	100.00	-100.00	-100.00
#1	1.5E-5	99.99	100.02	-100.07	-99.95
#2	6.4E-7	100.02	99.87	-99.68	-100.22
#3	1.2E-2	100.00	100.00	-100.00	-100.00
#4	6.9E-6	100.07	99.82	-99.77	-100.11
#5	1.2E-9	96.39	110.87	-115.84	-91.39

Table 2. Results for different number of sensors

Number of sensors	u_1 (%)	u_2 (%)	U (%)
6	0.5E-3	0.73	1.4
8	0.5E-3	0.28	0. 56
12	0.4E-3	0.	0.30

Table 3. Results for different number of sensors in presence of a stray field

Number of sensors	u_1 (%)	u_2 (%)	U (%)
8	0.7E-3	0.48	0.96
12	0.4E-3	0.16	0.32

5 DISCUSSION

The results obtained in the applications of the proposed method lead to the following considerations:

- the capability of the proposed procedure of correctly reconstructing the current (or mmf) values is determined

by the numerical characteristics of the algebraic system to be solved. The possibility of obtaining some matrix rows which are close to be linearly dependent can make the solution inconsistent;

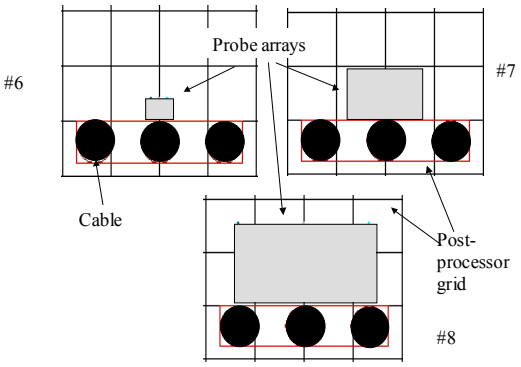

Fig. 2. Probe arrangement with respect to the cables: configuration #6, #7 and #8

Table 4. Results for 12 sensor array

Case	Without Stray Field			With Stray Field		
	u_1 (%)	u_2 (%)	E (%)	u_1 (%)	u_2 (%)	E (%)
#6	1.6E-3	0.97	1.9	2.2E-2	6.3	13
#7	2.7E-4	0.14	0.28	6.6E-4	0.26	0.52
#8	1.0E-4	0.10	0.20	1.0E-4	0.10	0.20

• the numerical characteristics of the matrix depends on the sensor positioning around the sources;

• the "quality" of the position of the probe array is expressed through a position index *PI* which quantifies the algebraic system characteristics.
IP allows comparisons among different positions of the same sensor array around the same source;

• uncertainty $\boldsymbol{u_2}$ due to the sensor accuracy is the predominant component;

• uncertainty $\boldsymbol{u_1}$, has been found always negligible with respect to $\boldsymbol{u_2}$;

• the stray field effect can be cut down increasing the *PI* and the sensor number.

6 CONCLUSIONS

The results, provided by the numerical simulations of the proposed procedure, are quite promising for a future implementation of the method in an experimental device. In this case, the algebraic coefficients of the system matrix defined in Sect. 2.1 should be evaluated by means of a suitable calibration procedure. Moreover the computational procedure here presented will be useful in order to define the best arrangement of the sensor array depending on the source geometry, the stray field, the sensor accuracy, dimension and number.

REFERENCES

[1] PRESS W.H., FLANNERY B.P., TEUKOLSKY S.A., VETTERLING W.T., Numerical Recipes, Cambridge University Press 1989 – pp. 52-64

[2] BOTTAUSCIO, O. - CHIAMPI, M. - CROTTI, G. - ZUCCA, M.: Influence of probe size on the measurement accuracy of non uniform ELF magnetic fields, to appear on Radiation Protection Dosimetry

Received 28 October 2004